ANTIOXIDANTS & REDOX SIGNALING
Volume 12, Number 6, 2010

DOI: 10.1089/ars.2009.2461

ORIGINAL RESEARCH COMMUNICATION

Activation of Membrane NADPH Oxidase Associated with Lysosome-Targeted Acid Sphingomyelinase in Coronary Endothelial Cells

Jun-Xiang Bao, Si Jin, Fan Zhang, Zheng-Chao Wang, Ningjun Li, and Pin-Lan Li

Abstract

This study explored the mechanism mediating the aggregation of membrane NADPH oxidase (NOX) subunits and subsequent activation of this enzyme in bovine coronary arterial endothelial cells (CAECs). With confocal microscopy, we found that FasL stimulated lipid rafts (LRs) clustering with NOX subunit aggregation and acid sphingomyelinase (ASM) gathering, which was blocked by the siRNA of sortilin, an intracellular protein responsible for the binding and targeting of ASM to lysosomes. Correspondingly, FasL-induced $O_2^{\cdot -}$ production through NOX in LRs fractions was abolished by sortilin siRNA. Further, with flow-cytometry and fluorescence resonance energy transfer (FRET) analysis, we surprisingly demonstrated that after FasL stimulation, sortilin was exposed to cell membranes from lysosomes together with Lamp-1 and ASM, and these lysosomal components were aggregated and form a signaling complex in cell membranes. With co-immunoprecipitation, lysosomal sortilin and ASM were found to interact more strongly when CAECs were stimulated by FasL. Functionally, inhibition of either sortilin expression, lysosome function, LRs clustering, or NOX activity significantly attenuated FasL-induced decrease in nitric oxide (NO) levels. It is concluded that lysosome-targeted ASM, through sortilin, is able to traffic to and expose to cell-membrane surface, which may lead to LRs clustering and NOX activation in CAECs. *Antioxid. Redox Signal.* 12, 703–712.

NAD(P)H OXIDASE (NOX) is emerging as an important redox-signaling enzyme. Its activation importantly relies on the assembling and aggregation of several subunits, including its membrane-associated subunits $gp91^{phox}$ or its isoforms and $p22^{phox}$, as well as cytosolic subunits $p47^{phox}$, $p40^{phox}$, $p67^{phox}$, and Rac (1). However, the mechanisms mediating such assembling or aggregation of NOX subunits to function as an active enzyme remain an unsolved problem. In particular, it is unknown what driving force leads to such activity of NOX on the cell membrane. Recently we reported that lipid rafts (LRs) clustering is an important mechanism determining the trafficking and aggregation of NOX subunits in the cell membrane of endothelial cells, which results in activation of NOX, constituting a membrane redox-signaling platform (11, 23, 28). We have no idea yet how such LRs-associated aggregation or assembling of NOX subunits occurs in these cells and what are the related regulatory mechanism and functional relevance of this NOX activation.

In this regard, we reported that lysosomal vesicles, which contain the ceramide-producing enzyme acid sphingomyelinase (ASM), play an important role in the formation of this redox-signaling pathway (9, 11, 27–29). ASM is a water-soluble, lysosomal glycoprotein that catalyzes the degradation of membrane-bound sphingomyelin into phosphocholine and ceramide (2, 15). This enzyme is synthesized in the Golgi apparatus, but it exerts its effect mainly in lysosomes, and therefore, many studies have been focused on how ASM is transferred from the Golgi apparatus to lysosomes (2, 6, 19, 30). Sortilin, a 95-kDa glycoprotein, has been classified as an enzyme that plays an important role in this transferring process (4, 16). Sortilin contains a Vps10p domain in its luminal region, which may be responsible for the binding to ASM and other proteins (18). The cytoplasmic tail of sortilin contains an acidic cluster–dileucine motif that binds to the monomeric adaptor protein GGA, a novel ubiquitous coat protein mediating the formation of intracellular-transport intermediates and selection of cargo (22). More recently, we demonstrated that sortilin-mediated targeting of ASM to lysosomes is of importance in LRs clustering because of the increase in ceramide production locally on the cell membrane (10). However, it remains unknown how sortilin is involved in the trafficking of ASM into the membrane and in the NOX

Department of Pharmacology & Toxicology, Medical College of Virginia Campus, Virginia Commonwealth University, Richmond, Virginia.

subunits assemblage and activation associated with LRs clustering. In addition, no evidence shows whether sortilin interacts with ASM, participating in the LR clustering and NOX-activation process.

In this study, we first determined the role of sortilin in the aggregation of NOX subunits, with $gp91^{phox}$ as a prototype, and in the activation of NOX with confocal microscopic localization of LRs-$gp91^{phox}$ and ASM complex in the cell membrane of CAECs and with analysis of $O_2^{\cdot-}$ production by using electromagnetic spin-resonance (ESR) spectrometry. Then we examined the behavior of sortilin during the process of LRs clustering by FasL stimulation, such as the measurement of sortilin and lysosome-marker exposure on the cell membrane by using flow cytometry, FRET detection between sortilin and related molecules in clustered LRs area, and analysis of interactions between sortilin and ASM in lysosomes during FasL stimulation. Finally, we addressed the possible functional relevance of such sortilin-mediated ASM trafficking and LRs clustering in the regulation of the endothelial NO level and bioavailability. All these experiments defined an important mechanism mediating NOX activation through sortilin and ASM trafficking into the cell membrane. The sortilin-ASM interaction and trafficking into the cell membrane leads to LRs clustering and assembling of NOX subunits, ultimately triggering NOX-mediated redox signaling or regulation in endothelial cells.

Materials and Methods

Cell culture

The primary cultures of bovine CAECs were obtained as we described previously (9–11, 27, 28). In brief, after the fresh bovine hearts were obtained, the epicardial circumflex and anterior descending coronary arteries were quickly dissected, placed in RPMI 1640, and cleaned of surrounding adherent fat and connective tissue. The lumens of arterial segments were filled with 0.25% collagenase A in RPMI 1640 supplemented with 0.1% bovine serum albumin (BSA) and incubated at 37°C for 15 to 30 min. The arteries were then flushed with RPMI 1640 supplemented with 2% antibiotic–antimycotic solution, 0.3% gentamicin, and 0.3% nystatin. Detached bovine CAECs were collected and maintained in RPMI 1640 supplemented with 20% FCS, 1% glutamine, and 1% antibiotic–antimycotic solution at 37°C in 5% CO_2. Isolated bovine CAECs were identified by morphologic appearance (*i.e.*, cobblestone array) and by positive staining for von Willebrand factor antigen. All biochemical studies were performed by using CAECs of two to four passages. According to some preliminary experiments and previous studies (10, 27, 28), the period of 15 min was applied for FasL stimulation to induce LRs clustering and to avoid other actions, such as apoptosis.

RNA interference

Sortilin siRNAs were purchased from INVITROGEN (CAT#HSS109429) which were confirmed to be effective in silencing sortilin gene in different cells by the company. Its efficiency in bovine CAECs has also been testified in our lab (10). The scrambled RNA has been confirmed as non-silencing double stranded RNA (10) and was used as control in the present study. Transfection of siRNA was performed using the QIAGEN TransMessenger tranfection kit (QIAGEN, Valencia, CA) according to the instruction manual.

Colocalization of LR clusters with acid sphingomyelinase or NADPH oxidase subunits in CAECs

For dual-staining detection of the colocalization of LRs with ASM or $gp91^{phox}$, the CAECs were first incubated with Al488-CTXB, as described previously (9, 11, 28), and then, as needed, with goat anti-ASM polyclonal antibodies (Santa Cruz, Santa Cruz, CA; 1:200) or mouse anti-$gp91^{phox}$ monoclonal antibody (BD Biosciences, San Jose, CA; 1:200), which was followed by Texas red-labeled anti-goat or anti-mouse secondary antibody (Molecular Probes, Eugene, OR; 1:1,000), respectively. Then the colocalizations were visualized with confocal microscopy.

Electronic spin resonance detection of $O_2^{\cdot-}$

Electronic spin resonance (ESR) detection of $O_2^{\cdot-}$ was performed as described previously (9, 11, 27, 28). In brief, gently collected CAECs were suspended in modified Krebs/HEPEs buffer containing deferoxamine (100 μM, metal chelator). Approximately 1×10^6 CAECs were mixed with 1 m*M* spin-trap 1-hydroxy-3-methoxycarbonyl-2,2,-5,5-tetramethyl-pyrrolidine (CMH) in the presence or absence of 100 units/ml polyethylene glycol (PEG)-conjugated superoxide dismutase (SOD). The cell mixture loaded in glass capillaries was immediately analyzed with ESR (Noxygen Science Transfer & Diagnostics GmbH, Denzlingen, Germany) for production of $O_2^{\cdot-}$ per minute for 10 min. The ESR settings were as follows: biofield, 3,350; field sweep, 60 G; microwave frequency, 9.78 GHz; microwave power, 20 mW; modulation amplitude, 3 G; 4,096 points of resolution; receiver gain, 500; and kinetic time, 10 min. The SOD-inhibitable signals were normalized by protein concentration and compared among different experimental groups.

Flow-cytometric analysis of protein expression on cell membrane

The presence of LRs and the expression of $gp91^{phox}$, sortilin, Lamp-1, and ASM on the cell membrane were assessed with flow cytometry. As described previously (24), CAECs were harvested and washed with PBS, and then blocked with 1% BSA for 10 min at 4°C. After two washes, the pellet was added to 100 μl PBS and incubated with AlexaFluor 488 (Al488)-CTXB (the B subunit of cholera toxin, which binds to lipid raft-enriched GM1 ganglioside and has been widely exploited to visualize lipid rafts; BD Biosciences, San Jose, CA; 1:500); or the cells were incubated with a rabbit source of antibody for sortilin (Abcam, Cambridge, MA; 1:400), a mouse source of antibody for $gp91^{phox}$ (BD Biosciences; 1:200), Lamp-1 (BD Biosciences; 1:200), or ASM (Santa Cruz biotechnology, Santa Cruz, CA; 1:200) followed by incubation with FITC-labeled anti-rabbit secondary antibody (BD Biosciences; 1:500), or FITC labeled anti-mouse secondary antibody (BD Biosciences; 1:500). Stained cells were run on a Guava Easycyte Mini Flow Cytometry System (Guava Technologies, Hayward, CA) and analyzed with Guava acquisition and analysis software (Guava Technologies).

Fluorescence resonance energy transfer analysis

CAECs were first incubated with goat anti-ASM polyclonal antibody (Santa Cruz Biotechnology; 1:200) followed by

FITC-labeled anti-goat secondary antibody (Molecular Probes; 1:1,000) or just incubated with FITC-labeled anti-Lamp-1 (BD Biosciences; 1:200). Lamp-1 is a lysosomal marker protein belonging to a type 1 integral membrane protein and is highly expressed in lysosomal membranes (3). Then the cells were incubated with rabbit anti-sortilin polyclonal antibody (BD Biosciences; 1:200) followed by TRITC-labeled anti-rabbit secondary antibody (Molecular Probes; 1:1,000) and then visualized with a confocal microscope (Olympus, Tokyo, Japan). To detect the FRET between ASM and Lamp-1, the cells were incubated with FITC-anti-ASM and TRITC-anti-Lamp-1. An acceptor bleaching protocol was used to measure the FRET efficiency, as we described previously (8, 9, 11, 28). After the prebleaching image was normally taken, the laser intensity at the excitement wavelength of the acceptor (TRITC) was increased from 50 to 98% and continued to excite the sample for 2 min to bleach the acceptor fluorescence. After the intensity of the excitement laser of the acceptor was adjusted back to 50%, the postbleaching image was then taken. A FRET image was obtained by subtraction of the prebleaching image from the postbleaching image and given a dark blue color. After measuring the FITC fluorescence intensity in the pre-, post-, and FRET image, the FRET efficiency was calculated through the following formula:

$$E = (\text{FITCpost} - \text{FITCpre})/\text{FITCpost} \times 100\%$$

Measurement of sortilin and acid sphingomyelinase interaction through co-immunoprecipitation

The lysosomes from CAECs were isolated with a lysosome isolation kit (Sigma, St. Louis, MO). In brief, the cells were grown to 90% confluence, and then trypsinized and washed. After homogenizing, the lysates were centrifuged at 1,000 *g* for 10 min, followed by 20 min at 20,000 *g*, to get crude lysosome fractions (CLFs). Then the CLFs were further purified and enriched on a density gradient. Finally, the isolated lysosomes were determined by measuring acid phosphatase activity and were ready for use (25).

Co-immunoprecipitation was performed with a Mammalian Co-immunoprecipitation Kit (Pierce Biotechnology, Rockford, IL) according to instructions of manufactory's manual. In brief, a mouse anti-ASM monoclonal antibody (Santa Cruz Biotechnology; 1:200) was first immobilized on the coupling gel beads and then incubated with lysosomes for 2 h. After being eluted and regenerated, the immunocomplexes were inactivated and prepared for electrophoresis. Immunoblotting was performed by using anti-ASM and anti-sortilin, respectively.

In situ simultaneous measurement of $[Ca^{2+}]_i$ and nitric oxide production in intact endothelium of coronary arteries

Ca^{2+} release and NO production induced by bradykinin (Sigma; BK, 1 μM) were detected with a method described previously (26). In brief, after loading the arteries with DAF-2 DA (Invitrogen, Carlsbad, CA; 10 μM) and fura 2-AM (Invitrogen, Carlsbad, CA, 10 μM), individual endothelial cells were visualized with an inverted microscope (Nikon, Melville, NY). Fluorescence images were recorded by a digital camera (SPOT RT Monochrome; Diagnostic Instruments, Sterling Heights, MI). Metafluor imaging and analysis software (Universal Imaging, Ypsilanti, MI) was used to acquire, digitize, and store the images and data for off-line processing and statistical analysis. $[Ca^{2+}]_i$ was calculated by using the following equation:

$$[Ca^{2+}]_i = K_d \beta [(R - R_{min})/(R_{max} - R)]$$

where K_d is 224 nM; R is the fluorescence ratio (F340/F380); R_{max} and R_{min} are the maximal and minimal fluorescence ratios; and β is the fluorescence ratio at 380-nm excitation determined at R_{min} and R_{max}, respectively. NO production was expressed as the net increment of DAF-2 fluorescence relative to its basal value ($f = \Delta F/F_0 \times 1{,}000$), where f is the net fluorescence; F is the DAF-2 fluorescence intensity obtained during experiments, and F_0 is its basal fluorescence intensity.

Statistics

Data are presented as mean ± SEM. Significant differences between and within multiple groups were examined by using ANOVA for repeated measures, followed by Duncan's multiple-range test. A value of $p < 0.05$ was considered statistically significant.

Results

Effects of sortilin gene silencing on acid sphingomyelinase trafficking and aggregation of NADPH oxidase subunits

RNA interference strategy was used to knock down sortilin gene expression. The efficiency of siRNA used by us has been proven before (10) and also was shown in Supplemental Fig. 1 (Supplemental Fig. 1; see www.liebertonline.com/ars) of the online supplemental materials. As shown in panel A of Fig. 1, FasL stimulated LRs clustering (green patches with Al488-CTXB) accompanied by translocation of ASM into these LR clusters, whereas control cells showed only some diffuse staining of both antibodies. When the sortilin gene was silenced, FasL-induced LR clustering and ASM translocation were blocked (siRNA + FasL). However, scrambled sRNA had no effect on FasL-induced LR clustering and ASM translocation (Scra + FasL).

It was reported that NOX subunits localized in LRs are an important feature of LR-redox signaling platforms (11, 14, 23, 28). As shown in panel B of Fig. 1, we demonstrated that in FasL-stimulated cells, fluorescent patches were identified by LR markers, Al488-CTXB (green) and anti-$gp91^{phox}$ antibody, plus a Texas red secondary antibody (red). Yellow patches or dots in the overlaid image showed colocalization of $gp91^{phox}$ in LR clusters. In sortilin siRNA-transfected CAECs, however, FasL-induced LR clustering and colocalization of $gp91^{phox}$ changes were not detected. In scrambled sRNA-transfected cells, FasL was still able to stimulate LR clustering and translocation of $gp91^{phox}$. In addition, we also found that siRNA of sortilin had similar effects to block the aggregation or translocation of $p47^{phox}$ into the LR clusters (not shown). Panel C of Fig. 1 summarized data showing that, after FasL stimulation, the percentage of LRs colocalized with ASM or $gp91^{phox}$ increased significantly. These results further support the view that LR-redox signaling platform formation depends on sortilin-mediated ASM targeting to lysosomes.

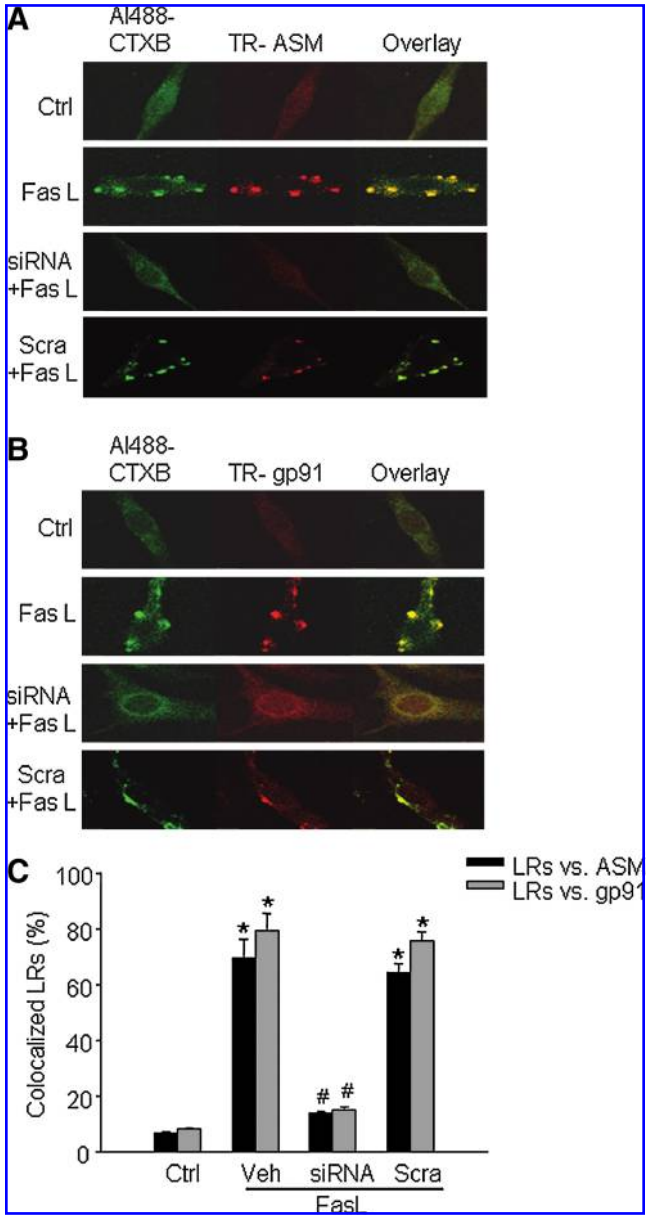

FIG. 1. Confocal microscopic analysis of colocalization of LR clusters and ASM or NOX subunits in CAECs. The cells were stained with Texas red–labeled anti-ASM (TR-ASM) or anti-gp91^{phox} (TR-gp91) antibody and LRs marker, Al488-CTXB. siRNA and Scra indicate sortilin siRNA and scramble sRNA transfection group, respectively. $^{*}p < 0.05$ *vs.* control group. $^{\#}p < 0.05$ *vs.* FasL group; $n = 6$ batches of cells.

Effects of sortilin gene silencing on NADPH oxidase activity

To determine the production of $O_2^{\cdot -}$ in the LR-NOX subunit complex, we examined the NOX activity by using ESR spectrometry. As summarized in Fig. 2, NOX activity, as indicated by $O_2^{\cdot -}$ production by NOX in FasL-stimulated CAECs (Veh), increased significantly compared with that in control (Ctrl). When these cells were transfected with sortilin siRNA, FasL failed to activate NOX in their membrane fractions (siRNA). This effect of sortilin siRNA was not observed in scrambled sRNA-transfected cells (Scra).

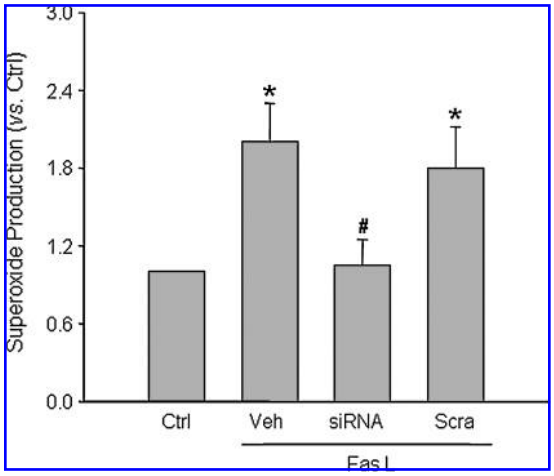

FIG. 2. Effects of sortilin siRNA transfection on FasL-induced $O_2^{\cdot -}$ production in CAECs measured with ESR spectrometry. Veh, vehicle group. $^{*}p < 0.05$ *vs.* control group. $^{\#}p < 0.05$ *vs.* FasL group; $n = 5$ batches of cells.

Detection of cell-membrane translocation of sortilin, Lamp-1, and acid sphingomyelinase

As shown in Fig. 3A, after stimulation with FasL, the frequency histogram of sortilin, Lamp-1, and ASM was right shifted to higher fluorescence intensity, suggesting recruitment of these proteins into the cell membrane. Conversely, the frequency histogram of gp91^{phox} and CTXB was at a high level under control conditions and did not move after FasL stimulation. This indicates that these membrane molecules are already present on the cell membrane, and no further increase occurs during FasL increase. Figure 3B summarizes data to show the percentage of positive-staining cells, which indicate the presence of LRs and expression of gp91^{phox}, sortilin, Lamp-1, and ASM on the cell membrane. FasL did not change the percentage of LRs and gp91^{phox}-positive cell populations, as compared to control, but induced a significant increase in the percentage of sortilin, Lamp-1, and ASM positive-staining cells. It appears that, after the activation of Fas, all three lysosomal proteins, including sortilin, Lamp-1, and ASM, are translocated to the cell membrane.

Detection of close relations among sortilin, acid sphingomyelinase, and Lamp-1

As shown in Fig. 4, CAECs were stained with FITC-labeled anti-Lamp-1 or anti-ASM antibody and TRITC-labeled anti-sortilin antibody. On the left, a control cell underwent an acceptor-bleaching protocol, and both pre- and postbleaching images were taken. The FRET image (in blue) was generated through the subtraction of the prebleaching image from the postbleaching image. On the right, a FasL-stimulated cell underwent the same FRET protocol. The aggregated sortilin and Lamp-1 or ASM on the cell membrane are shown in the overlay image on the top, and these colocalized molecules produced FRET, as shown in enhanced intensity of blue images on the bottom. Figure 5 summarizes the data from these experiments, which showed that FasL significantly increased the FRET efficiency between sortilin and Lamp-1 or ASM when they aggregated on the cell membrane. As shown in Figs. 4C and 5, we also examined the FRET efficiency between

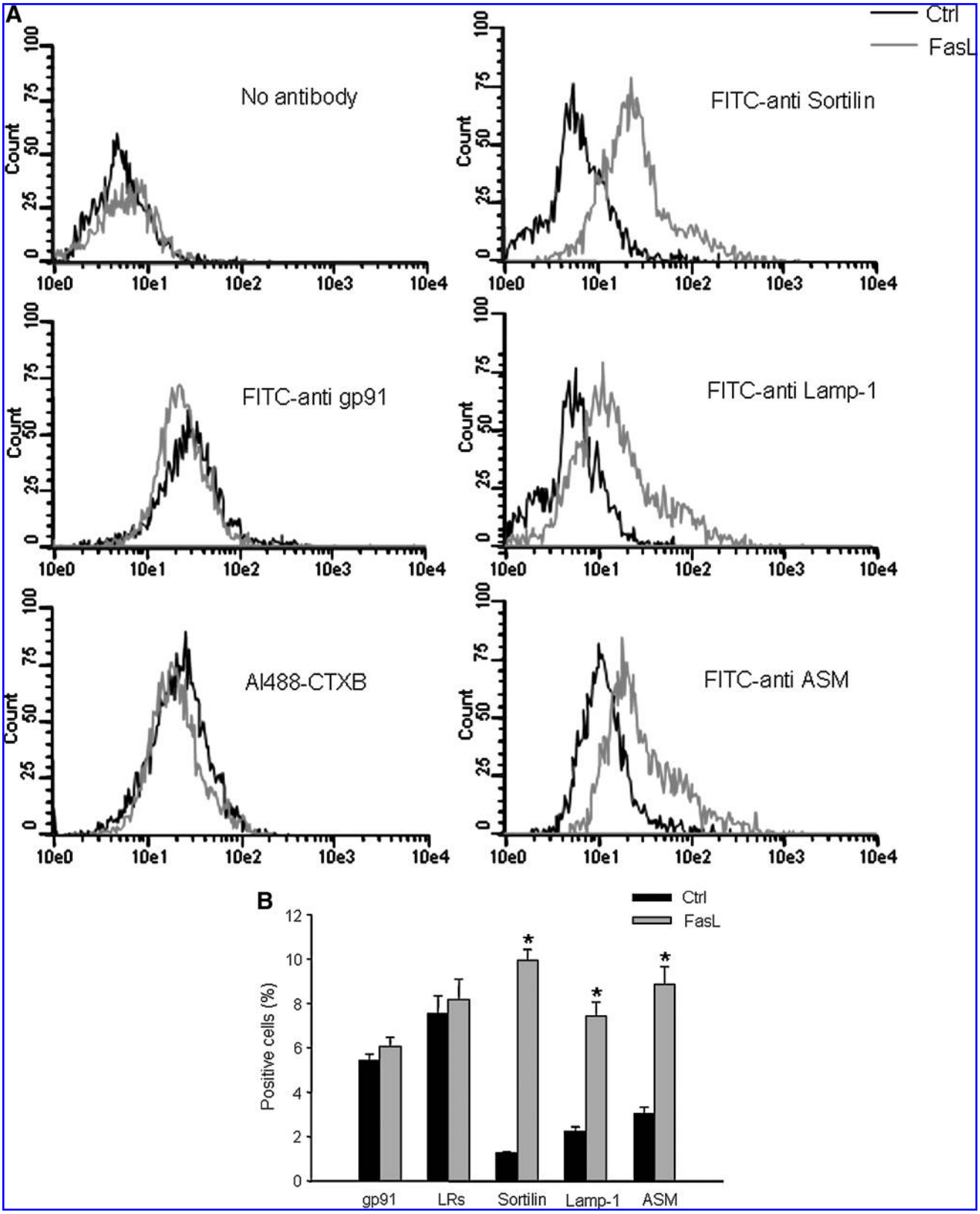

FIG. 3. Detection of sortilin, Lamp-1, and ASM on cell membrane in CAECs with flow cytometry. Control or FasL-stimulated (10 ng/ml for 15 min) cells were stained with FITC-labeled anti-gp91^{phox}, sortilin, Lamp-1, and ASM and analyzed with flow cytometry. AI488-CTXB was also used to detect LRs level on the cell membrane. *$p < 0.05$ *vs.* control group; $n = 4$ batches of cells.

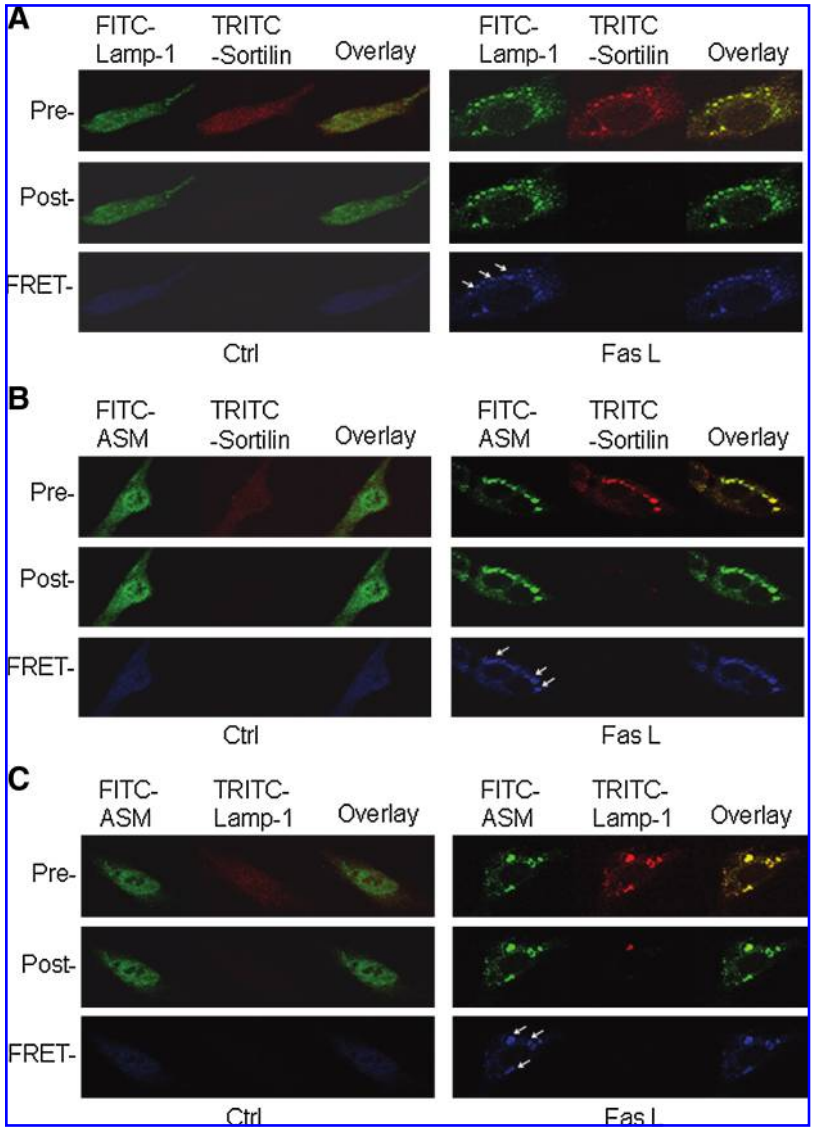

FIG. 4. Representative images of FRET analysis among sortilin, Lamp-1, and ASM in CAECs. The left group of images was obtained from control CAECs, and the right group of images, from FasL-stimulated (10 ng/ml for 15 min) cells. FRET was detected by using an acceptor-bleaching protocol. The blue images (representing FRET) on the bottom were obtained by subtracting a prebleaching image from a postbleaching image. *Arrows*, where the FRET happened. (**A**) FRET between Lamp-1 and sortilin. (**B**) FRET between ASM and sortilin. (**C**) FRET between ASM and Lamp-1.

ASM and Lamp-1, which became greater after FasL stimulation as compared with that in the control cell. It appears that after activation of the death receptor Fas, ASM and sortilin were closely trafficking together and targeted to lysosomes.

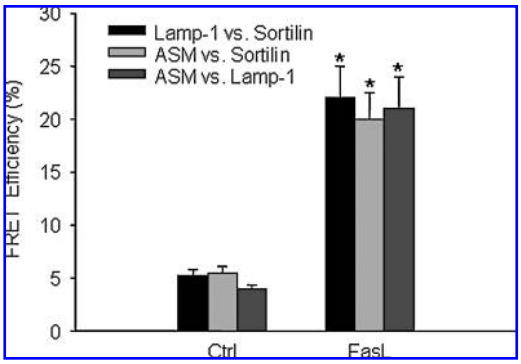

FIG. 5. Summarized results of detected FRET efficiency among sortilin, Lamp-1, and ASM. $^*p < 0.05$ *vs.* control group; $n = 5$ batches of cells.

Interaction of sortilin with acid sphingomyelinase in lysosomes

To test whether sortilin interacts with ASM during FasL treatment, we performed co-immunoprecipitation experiments to determine the changes in lysosomal sortilin when the reactive lysosomes were immunoprecipitated by using an anti-ASM antibody. As shown in Fig. 6A, the expression of sortilin (~95 kDa) or ASM (~70 kDa) was detected in the lysosomes from CAECs under control conditions (No-IP), and FasL stimulation did not change the sortilin level. After immunoprecipitation, it was found that FasL markedly increased the sortilin level, which was coeluted with anti-ASM antibody at the ASM level in elutes. In addition, an anti-sortilin antibody–recognized band at ~30 kDa may be the degrading product of this protein, which remained to be determined. Figure 6B is the summarized data showing that no significant difference was found in the expression of sortilin or ASM between control and FasL-treated cells in regular lysosomes. After immunoprecipitation with anti-ASM, the sortilin level was significantly increased when CAECs were stimulated by FasL.

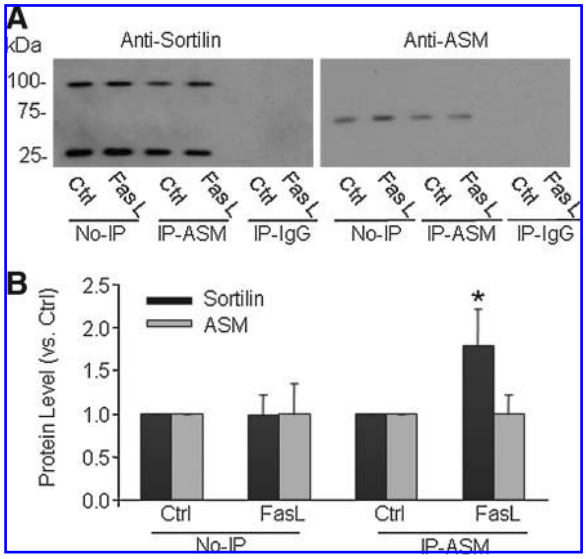

FIG. 6. Interaction of sortilin and ASM in lysosomes of CAECs detected with co-immunoprecipitation. $^*p < 0.05$ *vs.* control group; $n = 5$ batches of cells. Ctrl, control; FasL, FasL stimulation; No-IP, no immunoprecipitation conducted; IP-ASM, immunoprecipitation with beads conjugated with anti-ASM antibody.

Reversal of FasL-decreased NO level by sortilin siRNA, bafilomycin A1 (Baf), methyl-β-cyclodextrin (MCD) or gp91ds-tat

Ca^{2+} release and NO production induced by bradykinin (BK) were determined in isolated small bovine coronary arteries before and after FasL treatment. Figure 7 shows that BK may increase $[Ca^{2+}]_i$ (A) and induce NO production (B) in the intact endothelium of these isolated perfused arteries. The addition of FasL (10 ng/ml for 15 min) did not change Ca^{2+} release induced by BK, but markedly attenuated an increase in NO level in response to BK. Sortilin siRNA transfection, Baf (a lysosome-function inhibitor), MCD (a LR disruptor), or gp91ds-tat (a NOX inhibitor) blunted the action of FasL significantly. It was found that FasL attenuated a BK-induced increase in NO levels in the arterial endothelium by 70.8%. When these arteries were pretreated with sortilin siRNA, Baf, MCD, or gp91ds-tat, this action of FasL on BK-induced increase in NO level was blunted by 16.9%, 32.3%, 35.4%, and 15.4%, respectively. Scrambled sRNA transfection had no effect on this FasL-induced reduction in the NO level.

Discussion

The present study demonstrated that sortilin trafficked with ASM together into the cell membrane during death-receptor activation in CAECs, which may trigger the formation of the LRs-NOX membrane complex and thereby produce $O_2^{\cdot-}$, mediating redox signaling of such death-receptor activation. After the sortilin gene was silenced, FasL-stimulated LRs clustering and ASM translocation into LRs were blocked, and at the same time, the aggregation or translocation of NOX subunits into LRs clusters were prevented. We also confirmed that the sortilin-mediated formation of the LRs-NOX subunits complex exhibited NOX activity to produce $O_2^{\cdot-}$ in response to FasL stimulation and that silencing of the sortilin gene

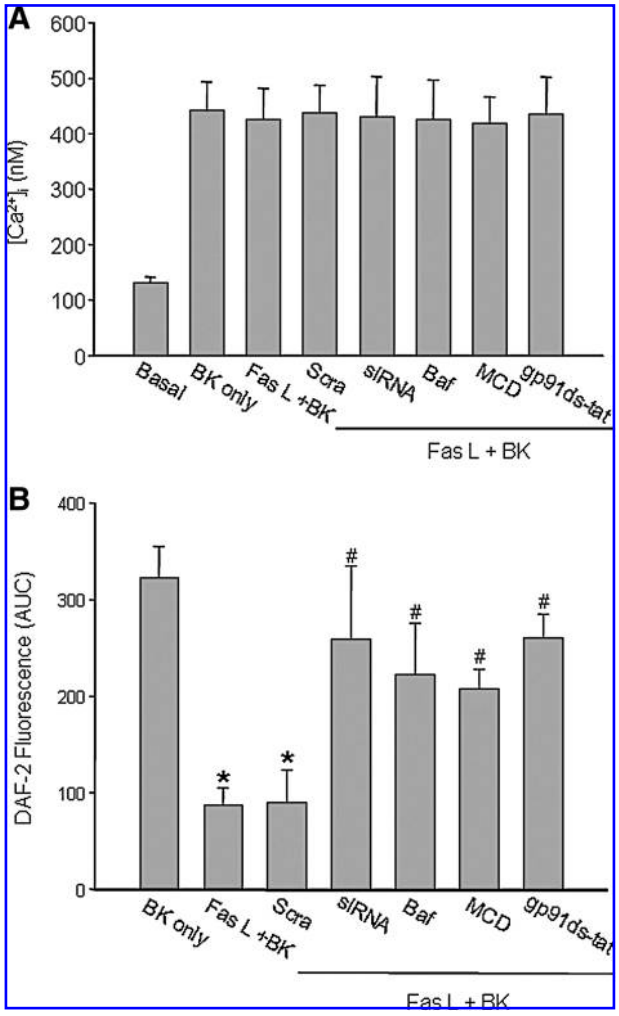

FIG. 7. Effects of FasL on BK-induced Ca^{2+} release (A) and NO production (B) in intact endothelium of bovine coronary artery before and after sortilin gene silencing, lysosome-function inhibition, LRs disruption, or NOX inactivation. BK (1 μM) was used to induce Ca^{2+} release and NO production in arteries with or without 20-min pretreatments with FasL (10 ng/ml) alone or FasL accompanied with sotilin siRNA or scramble sRNA transfection, Baf (100 nM), MCD (100 μM), or gp91ds-tat (50 μM). $^*p < 0.05$ *vs.* BK-only group; $^{\#}p < 0.05$ *vs.* FasL + BK group; $n = 5$ bovine hearts.

blocked $O_2^{\cdot-}$ production in the LRs fraction. Further analysis demonstrated that sortilin was exposed to the cell-membrane surface with ASM together, in response to FasL stimulation, which forms an integrative molecular complex in LRs areas. In addition, sortilin was found to interact with ASM, and such interaction was significantly enhanced during Fas activation. Functionally, sortilin-mediated trafficking and interaction with ASM were shown to play a critical role in FasL-induced impairment of NO bioavailability in the endothelium of intact small coronary arteries. Our results prove a hypothesis that sortilin trafficking and interaction with ASM importantly contribute to the activation of NOX in the redox regulation of coronary arterial endothelial function.

Increasing evidence suggests that LRs clustering is able to promote aggregation or translocation of NOX subunits and to form LR–redox-signaling platforms after death-receptor

activation (9, 11, 23, 27, 28). By using several different approaches, such as confocal microscopy and ESR analysis, the present study again demonstrated the formation of such LR–redox-signaling platforms, which were characterized by NOX subunits aggregation in LRs in response to Fas activation. In these platforms, NOX activity was significantly increased. Interestingly, after the sortilin gene was silenced, this NOX subunit aggregation in LRs induced by FasL was almost completely abolished. Correspondingly, FasL-enhanced NOX activity or $O_2^{\cdot-}$ production in the LRs fractions also was prevented by sortilin siRNA. These results suggest that the LR clustering associated with sortilin function serves as a driving force to result in the assembling or activation of NOX subunits to form an active enzyme on the endothelial cell membrane. To our knowledge, the present study for the first time links an intracellular molecular transporter, sortilin, to the formation of membrane LR clusters and to the NOX-mediating redox signaling in endothelial cells.

It is generally accepted that activation of the ASM by agonists or stimuli correlates with a translocation of this enzyme from intracellular stores onto the extracellular leaflet of the cell membrane (7, 14). This translocation may result in hydrolysis of sphingomyelin by ASM and the production of ceramide. Ceramide has been demonstrated to be induced in response to different injurious factors, especially those apoptotic factors including FasL, TNF-α, and endostatin. It leads to activation of NOX, producing endothelial dysfunction in small coronary arteries through the activation of LRs clustering and forms ceramide-enriched membrane platforms (7, 14, 28, 29). During the formation of these ceramide-enriched membrane platforms, different membrane proteins, enzymes, or signaling molecules can be aggregated, and some molecules in cytosol recruited to the membrane, which may result in a bulk amplification of the signals from related receptors. The present study confirmed FasL as a stimulus to activate such an LRs-clustering process, which led to assembling of NOX subunits and aggregation of other related molecules and thereby activated redox signaling in FasL response; this process is linked to the sortilin-associated molecular targeting and trafficking. In our previous studies, we provided evidence that ASM activation and translocation into the endothelial membrane can be attributed to lysosome trafficking and fusion to LR platforms in the cell membrane (10). The present study further demonstrates that the integrity of sortilin function is critical to the LR clustering, NOX-subunit assembling, and NOX activation. This for the first time suggests that an intracellular transporter directly participates in the activation of NOX in endothelial cells and thereby contributes to transmembrane signaling of the death-receptor activation. Previously, some reported that in fibroblasts from patients with mucolipidosis II (I-cell disease), ASM was released into the media in large quantities, which could be explained by the translocation of sortilin to the plasma membrane and the dissociation and release of bound ASM (16). Although these studies did not analyze membrane sortilin and ASM associated with LRs clusters and NOX subunits, the findings also suggest that sortilin plays an important role in the translocation of intracellular molecules into the cell membrane.

Next, we tested how sortilin works to facilitate the aggregation of NOX subunits. We first tried to address whether this intracellular transporter is directly involved in LRs clustering. With flow cytometry, a sensitive and widely used method (24) to analyze protein level on the cell membrane in nonpermeabilized cells, we found that, after FasL stimulation, the positive-stained cells with LRs marker CTXB and anti-gp91^{phox} antibody were stained even before FasL stimulation. When the cells were incubated with FasL, no difference was noted in the level of these two molecules. This suggests that LRs and gp91^{phox} are present in the cell membrane, and that FasL only induces clustering or aggregation, as we detected with confocal microscopy. In contrast, we found that positive cells stained with antibodies against three lysosomal proteins, sortilin, Lamp-1, and ASM, were very few under control conditions, but were significantly increased when the cells were stimulated by FasL. Such exposures of sortilin and ASM to the cell-membrane surface tell us that sortilin not only mediates targeting of ASM to the lysosomes, but also contributes to translocation of ASM into the plasma membrane with aggregation of various membrane molecules, such as GM1 and gp91^{phox}, in LR areas. This is further confirmed by blockade of NOX subunits aggregation by sortilin siRNA. More interestingly, fluorescence resonance energy transfer (FRET) analysis showed that sortilin, ASM, and Lamp-1 are very closely located when they are translocated into the cell-membrane LRs areas given strong FRET efficiency. This suggests that these molecules with clustered membrane components such as GM1 and NOX subunits forms an LR-protein complex, functioning as a signaling platform. During FasL stimulation, such a lysosome-membrane molecular complex will produce redox regulation of cellular function in CAECs.

With co-immunoprecipitation, we further investigated the interaction of sortilin and ASM in these CAECs. It was found that sortilin indeed interacts with ASM in lysosome preparations, as shown in co-immunoprecipitation of sortilin and ASM when we used only anti-ASM antibody-conjugated gel beads to react with lysosomes. FasL stimulation significantly enhanced such an interaction of sortilin and ASM. These findings further support the view that sortilin and ASM interact and are translocated together into the cell membrane during FasL stimulation, in which ASM is activated to produce ceramide, resulting in clustering of ceramide-enriched microdomains, a special form of LRs on endothelial cell membrane (13). In previous studies, two isoforms of ASM were reported in endothelial cells, one being secretory and another being lysosomal. They are encoded by one gene and a single mRNA, but undergo different posttranslational modifications in the Golgi apparatus (20, 21). Lysosomal ASM must be transferred to late endosomes and lysosomes after being synthesized (20). Sortilin, which is a 95-kDa glycoprotein, has been reported to play an important role for targeting or transferring of ASM and other proteins to lysosomes (4, 12, 16). Its Vps10p domain in the luminal region may be the binding site for the spaposin-like motif of ASM, whereas the cytoplasmic tail of sortilin contains an acidic cluster–dileucine motif that binds the monomeric adaptor protein GGA and is structurally similar to the cytoplasmic domain of M6P. All of these structural features determine sortilin as an intracellular protein transporter responsible for the sorting of soluble hydrolases such as ASM to lysosomes (4, 16). Our results about colocalization of sortilin with lysosome proteins during death-receptor activation indicate that sortilin not only simply mediates the targeting of ASM to lysosomes, but also func-

tionally interacts with ASM. The coupled sortilin and ASM work together to promote LRs clustering and to activate NOX to produce $O_2^{\cdot-}$, mediating the redox regulation of cell function. Given the enhanced colocalization of ASM and LRs marker (9–11, 14, 28, 29), this targeted ASM could move into the LR clusters in the cell membrane to form signaling platforms through lysosome trafficking and fusion. Interestingly, this sortilin effect is specific to death-receptor activation, such as FasL stimulation, because LRs clustering induced by a cell-permeable ASM activator, phosphatidylinositol (PI) (15) could not be blocked by sortilin siRNA (Supplemental Fig. 2; see www.liebertonline.com/ars). This suggests that sortilin-mediated LRs clustering and NOX subunit aggregation are related to receptor-dependent transmembrane signaling in response to death-receptor activation.

To address the physiological significance of this sortilin-mediated ASM targeting and trafficking into membrane LR clusters, we examined the effects of sortilin siRNA, lysosome function inhibitor-bafilomycin, and NOX peptide inhibitor-gp91ds-tat on the NO level in the intact endothelium of isolated and perfused coronary arteries. It was found that FasL-induced blunting of the NO increase in response to BK without effect on intracellular Ca^{2+} change was reversed by sortilin siRNA pretreatment, which was similar to the effect of lysosome functional inhibition and NOX inactivation. This uncoupling of intracellular Ca^{2+} release and NO increase was confirmed to be associated with $O_2^{\cdot-}$-induced reduction of NO bioavailability (9–11, 27–29). These results indicate that death-receptor activation by FasL may lead to endothelial dysfunction by decreasing the NO level via a signaling cascade associated with sortilin-mediated ASM targeting, lysosome trafficking, and fusion to LR microdomains, and subsequent formation of membrane LR-redox platforms. In these LR-redox platforms, NOX is activated to produce $O_2^{\cdot-}$, which reduces NO bioavailability in CAECs. This sortilin-mediated response to FasL may represent an early event of endothelial injury during death-receptor activation. In our preparations, endothelial cells or coronary arteries were exposed to FasL stimulation for only a short time. If these cells are exposed to FasL for a longer time, however, the apoptotic response could be induced, and sortilin-mediated action may also participate in such programmed cell death in response to FasL. In some current studies, indeed, a strong decrease in FasL-induced apoptotic indexes was observed in the presence of neutralizing anti-sortilin antibody in a multiple myeloma cell line, U266. Fas-receptor activation during 24 h altered the pattern of sortilin expression in these cells with a membrane relocation (5). These studies also suggested that sortilin serves as a critical signaling factor in initiating cell apoptosis if the cells are exposed to FasL >24 h. In addition, it has been reported that sortilin may serve as a co-receptor and molecular switch, enabling neurons expressing the neurotrophin receptors Trk and p75NTR to respond to a pro-neurotrophin and to initiate proapoptotic rather than prosurvival actions. In the absence of sortilin, regulated activity of extracellular proteases may cleave the pro-peptide of nerve growth factor (proNGF) to mature nerve growth factor (NGF)-11, promoting Trk-mediated survival signals (17). Although these studies indicated that proNGF creates a signaling complex by simultaneously binding to p75NTR and sortilin, it remains unknown how such a signaling complex is formed. The findings of the present study provide a clue that such membrane-signaling complex may be associated with the formation of LR-signaling platforms.

In summary, the present study demonstrated that lysosomal sortilin and ASM interact and traffic into the cell membrane in CAECs when these cells are stimulated by FasL. This sortilin-mediated lysosomal ASM activity and LRs clustering may lead to assembling or aggregation of NOX subunits and thereby activate NOX to produce $O_2^{\cdot-}$, reducing the intracellular NO level and thereby reducing NO bioavailability. Our results indicate that sortilin as an intracellular transporter interacts with ASM, which triggers the trafficking of lysosomes and related molecules to the cell membrane to form the membrane signaling platforms or complex. This lysosome–plasma membrane signaling platform transmits the signals from death-receptor activation resulting in cell dysfunction through redox regulation at a very early stage.

Acknowledgment

This study was supported by grants from the National Institutes of Health (HL-57244, HL-75316, and DK54927). The first two authors contributed equally to this work.

Author Disclosure Statement

No competing financial interests exist.

References

1. Babior BM. NADPH oxidase. *Curr Opin Immunol* 16: 42–47, 2004.
2. Baranski TJ, Faust PL, and Kornfeld S. Generation of a lysosomal enzyme targeting signal in the secretory protein pepsinogen. *Cell* 63: 281–291, 1990.
3. Barrachina M, Maes T, Buesa C, and Ferrer I. Lysosome-associated membrane protein 1 (LAMP-1) in Alzheimer's disease. *Neuropathol Appl Neurobiol* 32: 505–516, 2006.
4. Canuel M, Lefrancois S, Zeng J, and Morales CR. AP-1 and retromer play opposite roles in the trafficking of sortilin between the Golgi apparatus and the lysosomes. *Biochem Biophys Res Commun* 366: 724–730, 2008.
5. Fauchais AL, Lalloue F, Lise MC, Boumediene A, Prud'homme JL, Vidal E, and Jauberteau MO. Role of endogenous brain-derived neurotrophic factor and sortilin in B cell survival. *J Immunol* 181: 3027–3038, 2008.
6. Glickman JN and Kornfeld S. Mannose 6-phosphate-independent targeting of lysosomal enzymes in I-cell disease B lymphoblasts. *J Cell Biol* 123: 99–108, 1993.
7. Gulbins E and Kolesnick R. Acid sphingomyelinase-derived ceramide signaling in apoptosis. *Subcell Biochem* 36: 229–244, 2002.
8. Jia SJ, Jin S, Zhang F, Yi F, Dewey WL, and Li PL. Formation and function of ceramide-enriched membrane platforms with CD38 during M1-receptor stimulation in bovine coronary arterial myocytes. *Am J Physiol Heart Circ Physiol* 295: H1743–H1752, 2008.
9. Jin S, Yi F, and Li PL. Contribution of lysosomal vesicles to the formation of lipid raft redox signaling platforms in endothelial cells. *Antioxid Redox Signal* 9: 1417–1426, 2007.
10. Jin S, Yi F, Zhang F, Poklis JL, and Li PL. Lysosomal targeting and trafficking of acid sphingomyelinase to lipid raft platforms in coronary endothelial cells. *Arterioscler Thromb Vasc Biol* 28: 2056–2062, 2008.

11. Jin S, Zhang Y, Yi F, and Li PL. Critical role of lipid raft redox signaling platforms in endostatin-induced coronary endothelial dysfunction. *Arterioscler Thromb Vasc Biol* 28: 485–490, 2008.
12. Lefrancois S, Zeng J, Hassan AJ, Canuel M, and Morales CR. The lysosomal trafficking of sphingolipid activator proteins (SAPs) is mediated by sortilin. *EMBO J* 22: 6430–6437, 2003.
13. Li PL and Gulbins E. Lipid rafts and redox signaling. *Antioxid Redox Signal* 9: 1411–1415, 2007.
14. Li PL, Zhang Y, and Yi F. Lipid raft redox signaling platforms in endothelial dysfunction. *Antioxid Redox Signal* 9: 1457–1470, 2007.
15. Linke T, Wilkening G, Lansmann S, Moczall H, Bartelsen O, Weisgerber J, and Sandhoff K. Stimulation of acid sphingomyelinase activity by lysosomal lipids and sphingolipid activator proteins. *Biol Chem* 382: 283–290, 2001.
16. Ni X and Morales CR. The lysosomal trafficking of acid sphingomyelinase is mediated by sortilin and mannose 6-phosphate receptor. *Traffic* 7: 889–902, 2006.
17. Nykjaer A, Lee R, Teng KK, Jansen P, Madsen P, Nielsen MS, Jacobsen C, Kliemannel M, Schwarz E, Willnow TE, Hempstead BL, and Petersen CM. Sortilin is essential for proNGF-induced neuronal cell death. *Nature* 427: 843–848, 2004.
18. Petersen CM, Nielsen MS, Nykjaer A, Jacobsen L, Tommerup N, Rasmussen HH, Roigaard H, Gliemann J, Madsen P, and Moestrup SK. Molecular identification of a novel candidate sorting receptor purified from human brain by receptor-associated protein affinity chromatography. *J Biol Chem* 272: 3599–3605, 1997.
19. Puertollano R, Aguilar RC, Gorshkova I, Crouch RJ, and Bonifacino JS. Sorting of mannose 6-phosphate receptors mediated by the GGAs. *Science* 292: 1712–1716, 2001.
20. Schissel SL, Keesler GA, Schuchman EH, Williams KJ, and Tabas I. The cellular trafficking and zinc dependence of secretory and lysosomal sphingomyelinase, two products of the acid sphingomyelinase gene. *J Biol Chem* 273: 18250–18259, 1998.
21. Schissel SL, Schuchman EH, Williams KJ, and Tabas I. Zn^{2+}-stimulated sphingomyelinase is secreted by many cell types and is a product of the acid sphingomyelinase gene. *J Biol Chem* 271: 18431–18436, 1996.
22. Takatsu H, Katoh Y, Shiba Y, and Nakayama K. Golgi-localizing, gamma-adaptin ear homology domain, ADP-ribosylation factor-binding (GGA) proteins interact with acidic dileucine sequences within the cytoplasmic domains of sorting receptors through their Vps27p/Hrs/STAM (VHS) domains. *J Biol Chem* 276: 28541–28545, 2001.
23. Touyz RM. Lipid rafts take center stage in endothelial cell redox signaling by death receptors. *Hypertension* 47: 16–18, 2006.
24. Varsano S, Rashkovsky L, Shapiro H, and Radnay J. Cytokines modulate expression of cell-membrane complement inhibitory proteins in human lung cancer cell lines. *Am J Respir Cell Mol Biol* 19: 522–529, 1998.
25. Wilcox WR. Lysosomal storage disorders: the need for better pediatric recognition and comprehensive care. *J Pediatr* 144: S3–S14, 2004.
26. Yi FX, Zhang AY, Campbell WB, Zou AP, Van Breemen C, and Li PL. Simultaneous in situ monitoring of intracellular Ca^{2+} and NO in endothelium of coronary arteries. *Am J Physiol Heart Circ Physiol* 283: H2725–H2732, 2002.
27. Zhang AY, Yi F, Jin S, Xia M, Chen QZ, Gulbins E, and Li PL. Acid sphingomyelinase and its redox amplification in formation of lipid raft redox signaling platforms in endothelial cells. *Antioxid Redox Signal* 9: 817–828, 2007.
28. Zhang AY, Yi F, Zhang G, Gulbins E, and Li PL. Lipid raft clustering and redox signaling platform formation in coronary arterial endothelial cells. *Hypertension* 47: 74–80, 2006.
29. Zhang DX, Yi FX, Zou AP, and Li PL. Role of ceramide in TNF-alpha-induced impairment of endothelium-dependent vasorelaxation in coronary arteries. *Am J Physiol Heart Circ Physiol* 283: H1785–H1794, 2002.
30. Zhu Y, Doray B, Poussu A, Lehto VP, and Kornfeld S. Binding of GGA2 to the lysosomal enzyme sorting motif of the mannose 6-phosphate receptor. *Science* 292: 1716–1718, 2001.

Address correspondence to:
Pin-Lan Li, M.D, Ph.D.
Department of Pharmacology and Toxicology
Medical College of Virginia
Virginia Commonwealth University
410 North 12th
Richmond, VA 23298

E-mail: pli@vcu.edu

Date of first submission to ARS Central, January 18, 2009; date of final revised submission, September 17, 2009; date of acceptance, September 17, 2009.

Abbreviations Used

ASM = acid sphingomyelinase
Baf = bafilomycin
BK = bradykinin
BSA = bovine serum albumin
CAECs = coronary arterial endothelial cells
CTXB = cholera toxin subunit B
FasL = Fas ligand
LR = lipid raft
$O_2c^{\cdot}-$ = superoxide
PBS = phosphate-buffered saline
PFA = paraformaldehyde
ROS = reactive oxygen species

This article has been cited by:

1. Si Jin , Fan Zhou , Foad Katirai , Pin-Lan Li . 2011. Lipid Raft Redox Signaling: Molecular Mechanisms in Health and DiseaseLipid Raft Redox Signaling: Molecular Mechanisms in Health and Disease. *Antioxidants & Redox Signaling* **15**:4, 1043-1083. [Abstract] [Full Text] [PDF] [PDF Plus]
2. M. Xia, C. Zhang, K. M. Boini, A. M. Thacker, P.-L. Li. 2011. Membrane raft-lysosome redox signalling platforms in coronary endothelial dysfunction induced by adipokine visfatin. *Cardiovascular Research* **89**:2, 401-409. [CrossRef]
3. Gayle Gordillo , Huiqing Fang , Hana Park , Sashwati Roy . 2010. Nox-4–Dependent Nuclear H2O2 Drives DNA Oxidation Resulting in 8-OHdG as Urinary Biomarker and Hemangioendothelioma FormationNox-4–Dependent Nuclear H2O2 Drives DNA Oxidation Resulting in 8-OHdG as Urinary Biomarker and Hemangioendothelioma Formation. *Antioxidants & Redox Signaling* **12**:8, 933-943. [Abstract] [Full Text] [PDF] [PDF Plus] [Supplementary material]